Improved Interval Prediction of Small-Amplitude Hunting of High-Speed Trains

Jing Ning, Mingkuan Fang, Duoying Wang, Chunjun Chen, and Huajiang Ouyang

***Abstract*—Hunting is an important factor in the safe operation of high-speed trains. Most techniques used for monitoring hunting aim at detecting hunting occurrence and some of them can deal with small-amplitude hunting. However, they do not provide information about evolution of small-amplitude hunting. The present work studies the evolution of small-amplitude hunting with the goal of predicting the occurrence of the hunting instability. An improved method contained multiple hidden for predicting the interval of the amplitude of small-amplitude hunting is proposed, which is improved via a two-level model. The method is computationally efficient and converges rapidly. Upon applying the proposed method to high-speed train data, the coverage probability of the resulting prediction interval is 100% and its normalized average width is 0.187, which means a higher coverage and smaller width than the interval predicted by existing methods. The confidence-level of the prediction is also high.**

***Index Terms*—High-speed trains; Small-amplitude Hunting instability; Interval prediction; Neural network; Lower upper bound estimation.**

I. INTRODUCTION

WITH the increasing demand for high-speed passenger transportation in China, it is crucial to ensure the healthy operation of high-speed trains [1-3]. The hunting stability is an important factor in the safe operation of high-speed trains. Due to the conicity of the wheelset profile, the wheelset moves laterally and yaws around the centerline of the running track, which is called the hunting motion [4-7]. When the train speed exceeds a critical value, the amplitude of the hunting motion further increases with increasing speed, which leads to the hunting instability [8-10].

At present, fault monitoring and diagnosis technology has attracted wide attention of relevant practitioners, and this attention has also been reflected in the field of high-speed trains to a certain extent [11]. In order to ensure the safety and reliability of high-speed train operation, some monitoring and diagnosis criteria are integrated in high-speed train to prevent its failure [12]. Currently, criteria for the hunting instability are not uniform [13-15]. In China, the criterion of hunting instability is determined by the lateral acceleration signal of the bogie. From the perspective of high-speed train structure, the bogie is the only channel connecting the body and the track [16], it can absorb vibration and minimize the impact of track irregularity and wear, so as to make high-speed trains run relatively safely and smoothly [17]. And its own operation status is closely related to the safe operation of high-speed trains, so the bogie operation signal can represent the operation status of high-speed trains to a certain extent. The signal-based analysis method is to realize fault monitoring and diagnosis through the relevant signals generated during the operation of the equipment, such as temperature, vibration, etc [18]. Specifically, according to the hunting instability criteria in China [19], if after 0.5~10 Hz bandpass filtering, the peak of the lateral acceleration signal of the bogie frame is greater than or equal to 8 m/s^2 for six or more consecutive measurements, then the hunting instability is established.

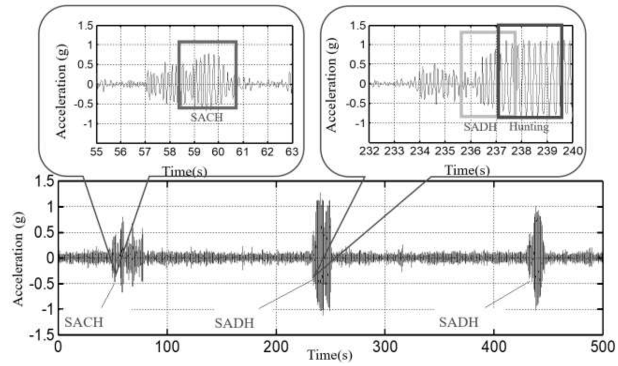

Fig. 1. Evolution of lateral acceleration for high-speed trains in a field test in China.

As shown in Fig. 1, the hunting instability encompasses three processes: normal operation, small-amplitude hunting (shown in the green and yellow boxes), and the hunting instability (shown in the red box). From the normal state, the train is subjected to small-amplitude hunting before reaching the hunting instability. Small-amplitude hunting may evolve in two ways: from small-amplitude hunting to the normal state (called "small-amplitude convergent hunting" SACH), which is safe for the train (shown in the green box), or from small-amplitude hunting to the hunting instability (called "small-amplitude divergent hunting", SADH), which tends to hunting (shown in the yellow box).

The evolution of small-amplitude hunting determines the occurrence of the hunting instability, which makes it vital to study the evolution of small-amplitude hunting to be able to

This research was funded by the National Natural Science Founda-tions of China, grant number 51975486 and 51975487 and was also supported by the Natural Science Foundation of Sichuan Province, grant number 2022NSFSC0398 (Corresponding author: Jing Ning).

Jing Ning, Mingkuan Fang, Duoying Wang, Chunjun Chen are with the School of Mechanical Engineering, Southwest Jiaotong University, Chengdu, 610031, Sichuan, China (e-mail: ningjing@swjtu.cn; 756140964@qq.com; wangduoying1021@qq.com; cjchen@swjtu.edu.cn).

Huajiang Ouyang is with the Center for Engineering Dynamics, School of Engineering, University of Liverpool, Liverpool, L69 3GH, Merseyside, UK (e-mail: h.ouyang@liverpool.ac.uk).

predict the hunting instability. Research into small-amplitude hunting has gradually developed over the years and is now attracting significant interest. With regard to the phenomenon of small, Souza a et al. [20] discovered its existence as early as 1986 when studying the hunting motion of freight car bogies and some researchers have referred to it in some literature [21, 22].

Qu et al. [23] combined experimental data and analyzed the signal characteristics of train bogie hunting. Sun et al. [24] pointed out that the criteria for judging the stability of lateral motion of high-speed trains in China cannot be used to detect small-amplitude hunting under supercritical bifurcation. An et al. [25] proposed an empty car swing alarm device. Through simulation analysis of the oscillation wavelength and acceleration of freight cars, it is proposed that the filtering frequency should be controlled between 0-15 Hz, and the recommended limit value for lateral acceleration of the frame is 0.6 g. Yao et al. [26] proposed an index to quantitatively evaluate the lateral stability of high-speed trains based on the root mean square of bogie lateral acceleration.

Gan et al. [27] designed a device that uses the Bayesian clustering algorithm for online monitoring of the stability of the lateral motion of high-speed trains. Zeng et al. [28] calculated the periodicity index of the phase trajectory of the lateral acceleration signal of the frame (i.e., car body or axle box) and set a threshold to determine the hunting state of high-speed trains. Sun et al. [29] identified the hunting state (including small-amplitude hunting and the hunting instability) of high-speed trains via a correlation analysis of the lateral acceleration of the car bodies and frames.

In this paper, the authors also do some preliminary research on the Small-Amplitude Hunting state monitoring by using machine learning method (References [30-33] present research on ways to identify small-amplitude hunting states based on the deep learning methods.) A Dempster-Sharer evidence theory-based approach for lateral running state recognition of high-speed trains was proposed by Ning et al. [30] after combining the empirical mode decomposition (EMD) artificial feature extraction method. A method called multi-scale alignment entropy local tangent space alignment was proposed by Ning et al. [31] to extract the non-smooth features of a signal. In order to measure small-amplitude hunting movements and reduce the complexity of feature data, a multi-scale alignment entropy local tangent space alignment method was proposed by Ning et al. [32]. To further improve the classification accuracy, Ye et al. [33] adopted an improved ensemble empirical mode decomposition method.

In short, existing methods mainly focus on the normal state and hunting instability, and a limited amount of literature discusses the evolution of small-amplitude hunting. This work studies the evolution of small-amplitude hunting to predict the occurrence of the hunting instability. The objective of the present study is to identify the small-amplitude hunting state and predict whether it will evolve into the hunting instability. The former is a classification problem, and the latter is a prediction problem.

By exploiting vibrational data, machine learning can be used to map the measured state variable feature space to the hunting-fault space to predict whether it will evolve from small-amplitude hunting into the hunting instability. But high-speed trains are complex nonlinear systems [34] that operate in a constantly changing environment, which means that the traditional point-prediction error is quite large, making it difficult to give a prediction confidence level. Therefore, we use herein an interval estimation method to predict the evolution of small-amplitude hunting.

For interval prediction, the computationally efficient lower upper bound estimation (LUBE) model, initially proposed by Khosravi et al. [35] in 2010, is based on neural networks that do not need a prior hypothesis distribution, and this method has been widely applied in various fields. Gan et al. [36] developed a new interval prediction method using time convolutional networks (TCN) within the LUBE framework and designed an interval width adaptive adjustment strategy to optimize the model by directly constructing training labels. This method can overcome the shortcomings of traditional methods that cannot be used to optimize interval prediction. In order to better quantify the uncertainty of landslide evolution, Lian et al. [37] proposed an advanced prediction interval construction method called $LUBE_{NCWC+pre\text{-}trained}$. It can directly construct prediction intervals by training neural networks without assuming data distribution in advance. The experimental results on seven benchmark datasets indicate that this method has certain advantages in generating high-quality prediction intervals. Chen et al. [38] proposed a new initialization method for solar power generation prediction interval model based on LUBE structure. This method initializes the input weight matrix of the LUBE model through an extreme learning machine automatic encoder (ELM-AE), and uses linear regression interval estimation (LRIE) to complete the initialization of the prediction interval, which has more detailed optimization and stable generalization performance. Li et al. [39] proposed a new wind speed interval prediction system based on LUBE, which to some extent overcomes the shortcomings of other LUBE models being unable to effectively learn the wind speed change patterns behind the data, as well as unstable performance. Its extraction of potentially important historical change patterns is based on an innovative parallel feature selection module and utilizes a forgetting operator as a feature constrained LUBE training algorithm. Lu et al. [40] developed a new method for predicting the range of carbon residual content of crude oil based on the upper and lower bound estimation LUBE method and combined it with a deep stochastic configuration networks (DSCN). Through these techniques, this method overcomes the disadvantage of slow neural network training process in early LUBE methods.

In recent years, there have been many studies on optimizing and improving LUBE. Ni et al. [41] proposed a new integrated method based on ELM and LUBE (ELUBE) to overcome the instability of Extreme Learning Machine (ELM) for short-term photovoltaic power prediction. This method significantly improves the quality of PI for photovoltaic power prediction five minutes in advance (in terms of clarity and coverage probability). Qi et al. [42] proposed a transformer top oil temperature interval prediction model based on kernel extreme learning machine (KELM) and Bootstrap method. This method can effectively consider the uncertainty of the transformer top oil temperature prediction model and obtain a more accurate and reliable top oil temperature prediction interval.Shi et al. [43] proposed the LUBE method based on the recurrent neural network (RNN) to directly construct the optimal PI for wind power prediction. The numerical results of real-world wind power datasets indicate that the proposed RNN prediction model can construct better PI compared to the benchmark model. Kavousi Fard et al. [44] proposed a new social spider optimization (SSO) based optimization method to construct the optimal PI in LUBE, which is characterized by its ability to utilize fuzzy logic theory and aggregation mechanisms to construct high-quality PI. [45] Lian et al. proposed a new hybrid method to construct high-quality PI for landslide displacement. This method is used to optimize bootstrap based PI and is later combined with neural network switching methods. For wind power/speed interval prediction, in order to achieve better efficiency and predictive performance, Liu et al. [46] designed an improved LUBE model using a new training scheme based on the gradient descent (GD) method. Peng et al. [47] proposed a new LUBE model based on gated recursive units for cluster wind power prediction. It completes interval prediction based on point prediction results and corresponding error intervals, and also utilizes GD to achieve optimized prediction reconstruction. For LUBE, the cost function currently available for uncertainty guided neural network training is not always convergent, and all converged neural networks have not generated optimized PI. In response to this issue, Kabir et al. [48] proposed a highly customizable smoothing cost function for developing neural networks to construct the optimal PI. Saeed et al. [49] integrated lower upper bound estimation method (LUBE) into a quasi-recurrent neural network, using which the network can be trained with conventional stochastic gradient descent.

Unfortunately, as noted in Ref. [37], "the LUBE method would cause several inevitable limitations, such as overtraining, high computation burden, and so on." Thus, the following issues remain to be addressed to optimize the LUBE method:

1) Multiple hidden layers are needed to solve complex problems. The traditional LUBE method uses only a single hidden layer. However, with a complex model, a good convergent solution cannot be obtained by simply using one hidden layer.
2) In a prediction interval task, the multiple hidden layers cannot be directly trained. The loss function of the prediction interval is obtained by discontinuous functions, which cannot be trained by a back-propagating algorithm. Thus, a heuristic algorithm must be used to train the loss function of prediction intervals. Unfortunately, heuristic algorithms are not optimal for multi-layer structures.

To resolve these issues, we propose herein an improved LUBE method called the two-level trained LUBE (TL-LUBE) method. In this method, the multiple hidden layers are pre-trained by the back-propagating algorithm, and the last layer is optimized by using a heuristic algorithm. In this way, various architectures can be used for the hidden layers of the TL-LUBE. This enables us to adjust the network architecture according to the requirements of the application so that the network may be applied to a wider range of applications.

So the evolution of small-amplitude hunting is studied to predict the occurrence of the hunting instability. And an improved method for predicting the interval of the amplitude of small-amplitude hunting is proposed.

Hunting is a serious obstacle to the high-speed operation of trains. All the monitoring systems are designed to detect hunting only after hunting has developed sufficiently. With the increasing speed of high-speed trains, it is an effective way to establish an accurate and fast warning system for hunting by predicting evolution trend of small amplitude hunting before the hunting phenomenon has developed sufficiently. If the train is classified as experiencing the hunting instability, an alarm will sound to remind drivers to reduce the train speed and avoid hunting. which will provide important support for an accurate and fast hunting warning system of high-speed trains. Based on the above problems, the authors propose a study on the prediction of small-amplitude hunting of high-speed trains. A TL-LUBE method is proposed to predict the evolution of the small-amplitude hunting state. This method offers high computational efficiency and rapid convergence.

This paper makes the following contributions:

1) An improved lower upper bound estimation model is proposed. The structure of the hidden layer and of the optimization algorithm is improved via a two-level model.
2) The improved model is used to predict the evolution of small-amplitude hunting, and the interval has higher coverage and smaller width.

II. Material and Methods

A. Traditional prediction intervals

This section introduces traditional prediction intervals (*PIs*). The *PI* coverage probability ($PICP$) and the *PI* normalized average width ($PINAW$) are evaluations of the *PI*. The parameters of the traditional LUBE model are optimized by using heuristic algorithms. The coverage-width-based criterion (CWC) is one of the loss functions of the heuristic algorithm [35].

$$PICP = \sum_{i=1}^{N} \delta_i / N \tag{1}$$

where N is the number of test samples and δ_i is a binary function defined as

$$\delta_i = \begin{cases} 1, & y_i \in [L(x_i), U(x_i)] \\ 0, & y_i \notin [L(x_i), U(x_i)] \end{cases} \tag{2}$$

where $L(x_i)$ and $U(x_i)$ are the upper and lower intervals of the output corresponding to sample i, respectively.

Once $PICP$ is defined, we must limit the width of the interval because the result is not practical if the width is too large. Therefore, the prediction interval average width ($PIAW$) is mathematically defined as

$$PIAW = \sum_{i=1}^{N} [U(x_i) - L(x_i)] / N \tag{3}$$

Next, $PINAW$ is defined as the normalized $PIAW$:

$$PINAW = PIAW/R \tag{4}$$

where R is a standard value of the dataset. Finally, the CWC is defined as

$$CWC = PINAW\left(1 + \gamma(PICP)e^{-\eta(PICP-\mu)}\right) \tag{5}$$

where $\gamma(PICP)$ is the binary function

$$\gamma = \begin{cases} 0, & PICP \geq \mu \\ 1, & PICP \leq \mu \end{cases} \tag{6}$$

with μ being the confidence.

B. Interpretation of TL-LUBE method

The traditional LUBE method [35] has only one hidden layer. However, when the model is complex, many parameters must be optimized: a good solution cannot be obtained by simply using a single hidden layer. The proposed TL-LUBE method thus contains multiple hidden layers (see Fig. 2).

The model has n hidden layers. The output of the i th hidden layer H_i is

$$\boldsymbol{H}_1 = g_1(\boldsymbol{X}\boldsymbol{W}_1 + \boldsymbol{b}_1) \tag{7}$$

$$\boldsymbol{H}_{i+1} = g_{i+1}(\boldsymbol{H}_i\boldsymbol{W}_{i+1} + \boldsymbol{b}_{i+1}),\ i \leq n-1 \tag{8}$$

where $\boldsymbol{W}_i$ is the weight of hidden layer i, $\boldsymbol{b}_i$ is the bias of hidden layer i, and g_i is the activation function of hidden layer i. The *PIs* are

$$[\boldsymbol{L}(x_i), \boldsymbol{U}(x_i)] = \boldsymbol{H}_n \times [\boldsymbol{\beta}_1, \boldsymbol{\beta}_2]^T \tag{9}$$

where $\boldsymbol{L}(x_i)$ and $\boldsymbol{U}(x_i)$ are the lower and upper intervals of the output corresponding to sample i, respectively, $\boldsymbol{H}_n$ is the output matrix of the last hidden layer, and $\boldsymbol{\beta}_1$, $\boldsymbol{\beta}_2$ are the weights of the output layer.

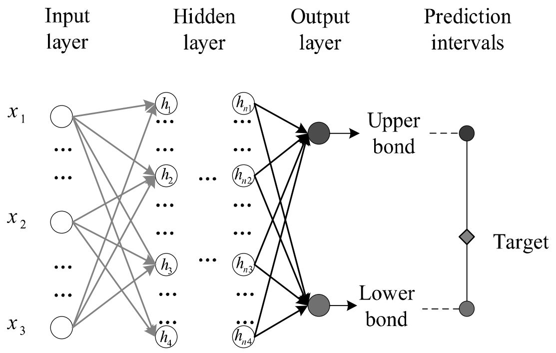

Fig. 2. Multiple hidden layers in the proposed TL-LUBE method.

When a model is complex and has many parameters, the heuristic algorithm cannot provide a rapid convergent solution. Thus, the LUBE model is divided herein into primary and secondary networks. Different loss functions are used for parameter optimization.

The loss function of the primary network is the mean square error (*MSE*) function:

$$MSE = \sum_{i=1}^{N}(y_i - \hat{y}_i)^2/N \tag{10}$$

where y_i is the target and $\hat{y}$ is the prediction. In the secondary network, a heuristic algorithm optimizes the remaining parameters. From Eq. (5), the loss function is CWC.

In short, the parameter optimization algorithm of the original LUBE model is improved via a two-level model, which improves the optimization efficiency.

C. TL-LUBE optimization method

As shown in Fig. 3, the TL-LUBE method is divided into primary and secondary networks. Such two-phase structures are all the CNN-RNN structures.

1) The primary network is a standard single-output prediction structure, which outputs only a single prediction. It uses gradient descent to train the parameters of the ANN layer. The loss function of the primary network is a continuous function.
2) The secondary network is a LUBE model, which outputs a prediction interval. It uses the heuristic dragonfly (DA) algorithm [50] to optimize the parameters of the output layer. The loss function of the secondary network is a discontinuous function.

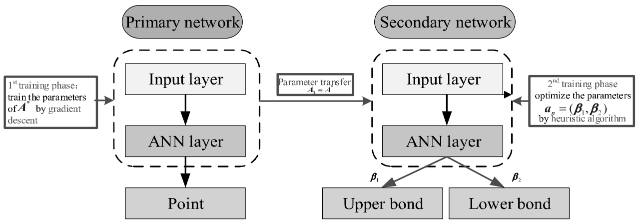

Fig. 3. Architecture of two-level network (primary and secondary networks).

The steps to train the TL-LUBE model are as follows:

1) Divide the data set constructed from the pre-processed raw data into training and test sets according to a chosen set ratio.
2) Input the data in the training set to the primary network, which is trained to obtain the parameters of the primary network weights.

The output of the primary network is $\hat{y}_i^*$ and the loss function of the primary network is

$$MSE = \sum_{i}^{N}(\hat{y}_i^* - y_i)^2/N \tag{11}$$

where y_i is the true peak of the sample in the time series, the asterisk $*$ indicates the parameter related to the primary network, ^ represents the output value of the network, $\hat{y}_i^*$ is the predicted peak of the sample in the time series output of the primary network, where the subscript i represents the true value of the peak or the point-prediction value, and N is the total number of point-prediction outputs.

Based on the loss function of the primary network, the primary network is trained by applying the BP algorithm until it converges, and the weight parameter matrix $\boldsymbol{A}^*$ of the primary network is obtained.

3) Import the trained network weight parameters obtained from the primary network into the secondary network to complete the setting of the weight parame-

ters of the secondary network.

4) Transform the point-prediction layer in the last layer of the secondary network into a prediction interval layer and then use its output as a confidence interval to obtain the secondary network. The primary network weight-parameter matrix $\boldsymbol{A}^*$ gives the initial value of the secondary network weight-parameter matrix $\boldsymbol{A}_0$, which is denoted as follows

$$\boldsymbol{A}_0 = \boldsymbol{A}^* = [\boldsymbol{a}_1^*, \boldsymbol{a}_2^*, \ldots, \boldsymbol{a}_{n-1}^*, \boldsymbol{a}_n^*] \tag{12}$$

where $\boldsymbol{a}_n^*$ is the weight parameter of layer n of the LUBE model. In the primary network, freeze all the network weight parameters that correspond to the initial value $\boldsymbol{A}_0$ of the weight parameter matrix except the last layer. The frozen network weight parameters $\boldsymbol{w}$ are given by

$$\boldsymbol{w} = [\boldsymbol{a}_1^*, \boldsymbol{a}_2^*, \boldsymbol{a}_3^* \ldots, \boldsymbol{a}_{n-1}^*] \tag{13}$$

Based on the frozen network weight parameters $\boldsymbol{w}$, the initial network weight-parameter matrix $\boldsymbol{A}_0$ of the LUBE model is

$$\boldsymbol{A}_0 = [\boldsymbol{w}, \boldsymbol{a}_n^*] \tag{14}$$

5) Optimize the final parameters of the secondary network by using the particle swarm optimization algorithm to obtain a trained LUBE model. Based on the output $\hat{y}_i$ of the secondary network, the trained LUBE model is obtained through the test set. The weight network parameter matrix $\boldsymbol{A}$ of the trained LUBE model is

$$\boldsymbol{A} = [\boldsymbol{w}, \boldsymbol{a}_n^*] \tag{15}$$

where $\boldsymbol{a}_n$ is the network weight parameter of layer n of the LUBE model optimized by using the secondary network.

In short, parameters $\boldsymbol{w} = [\boldsymbol{a}_1^*, \boldsymbol{a}_2^*, \boldsymbol{a}_3^* \ldots, \boldsymbol{a}_{n-1}^*]$ of the ANN layer trained in the primary network are reused as fixed parameters in the secondary network. In this way, only the parameters $\boldsymbol{a}_n$ of the output layer of the primary network require optimization by heuristic algorithms, which greatly reduces the number of parameters to be optimized in the secondary network.

The original optimization algorithm does not converge easily because the parameters of the model increase after changing the model from a single-layer ANN to a multi-layer ANN. Therefore, we propose a two-step optimization method. The proposed method divides the LUBE model into primary and secondary networks. The gradient descent algorithm is used to optimize the parameters of the primary network, and the DA is applied to optimize the parameters $\boldsymbol{\beta}_1$ and $\boldsymbol{\beta}_2$ of the last layer of the secondary network. Fig. 4 shows the two-step optimization process.

In the first training phase, part of the test data set is used to train the primary network.

1) The dataset is divided into two sub-datasets A and B, which are used to train the primary and secondary networks, respectively. Dataset A serves to train the primary network.
2) Initialize the precision (eps = 0.001) of the MSE loss function and the parameters of the primary network.
3) A dataset is input into the initial model to predict its sequence and calculate MSE.
4) If MSE < *eps*, the primary network training is fulfilled. Otherwise, the model parameters are trained by using the gradient descent algorithm, and the process returns to step (3).

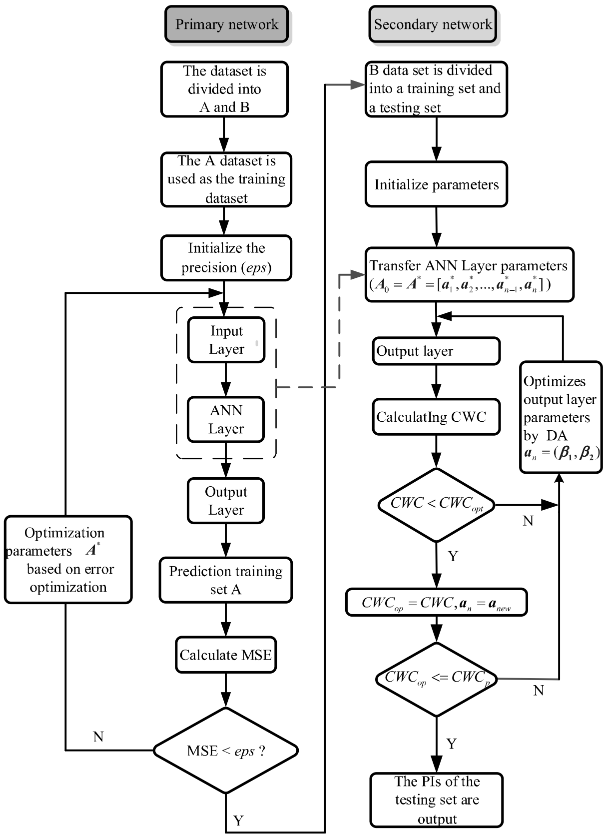

Fig. 4. Training flow chart.

In the second optimized phase, another part of the data is used to train the secondary network.

1) After completing the primary network optimization, dataset B is divided into training and testing sets.
2) Initialize the output layer parameters $\boldsymbol{a}_n = (\boldsymbol{\beta}_1, \boldsymbol{\beta}_2) = \boldsymbol{a}_n^*$, the expected value of the loss function ($CWC_p = 0.1$), and the optimal value of the loss function ($CWC_{op} = inf$).
3) The input and ANN layer parameters of the trained primary network are reused in the corresponding layer of the secondary network. Only the parameters of the output layer of the secondary network require training.
4) Input the training dataset into the model and calculate CWC.
5) If $CWC < CWC_{op}$, then $CWC_{op} = CWC$. Update the output layer parameters ($\boldsymbol{a}_n = \boldsymbol{a}_{new}$). Otherwise, apply the DA to optimize the parameters of the output layer, and go to step (4).

6) If $CWC_{op} \leq CWC_p$, the secondary network is trained and the PIs of the testing set are obtained. Otherwise, the output layer parameters are updated by using the DA, and the process returns to step (4).

III. Prediction of small-amplitude hunting

A. Dataset

A field tracking test was conducted to study hunting in high-speed trains. The dataset used in this paper is from the lateral acceleration of the bogie frame of a high-speed train moving at 320~350 km/h. Fig. 5 and Fig. 6 show the installation of the lateral accelerometer of the bogie frame S1, S2. Fig. 7 shows the velocity of the train, and Fig. 8 shows the corresponding lateral acceleration of the bogie frame. All data were acquired in strict compliance with China's Railway Passenger Traffic Safety Monitoring Standard [19].

The model of the accelerometer is LC0709A-18, and its range is 0-18 g, with a testing accuracy of 0.5%.

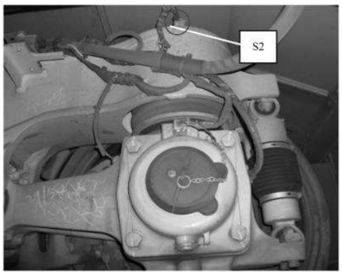

Fig. 5. Field installation of sensors

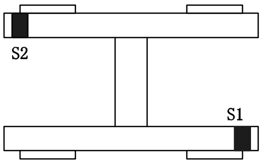

Fig. 6. Installation diagram of sensors (S1: Sensor 1, S2: Sensor 2)

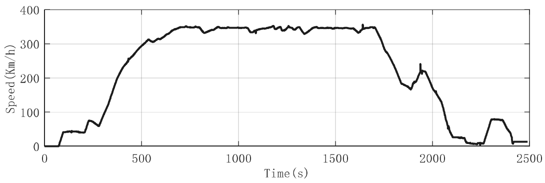

Fig. 7. Train velocity

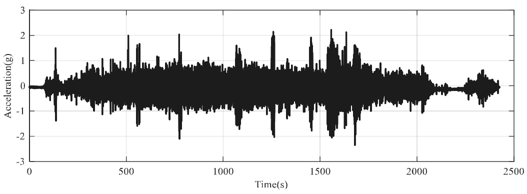

Fig. 8. Lateral acceleration of bogie frame

B. Definition of small-amplitude hunting

No strict definition of small-amplitude hunting is available in the literature. The hunting monitoring criteria currently used in China [19] are as follows: The hunting phenomenon exists when the lateral acceleration of the bogie frame exceeds 8~10 m/s^2 for more than six consecutive measurements after 0.5~10 Hz bandpass filtering. In addition, according to recent research [28, 29], when hunting occurs in high-speed trains (including hunting instability and small-amplitude hunting), the transverse acceleration signals of their frames and axle boxes are more periodic than during normal operation.

The Lyapunov functions of normal, small-amplitude hunting and hunting instability were calculated for the frame acceleration signals in the tracking data by using the Wolf-Lyapunov [51] algorithm. The functions appear in Fig. 9 and show that the signal is more periodic for hunting instability, followed by small-amplitude hunting. The normal signal is the least periodic due to its tendency to enter a random vibration state. This is consistent with Refs. 8 and 9, which indicate that the small-amplitude hunting state defined herein is reasonable.

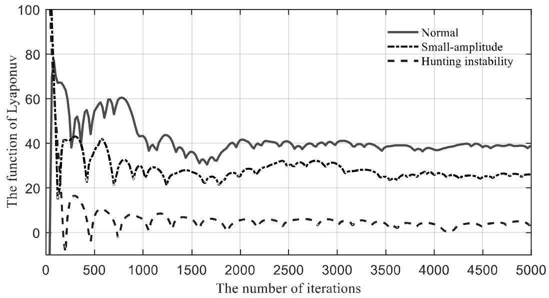

Fig. 9. Lyapunov functions calculated from frame acceleration signals of the tracking data

C. Input and output variable selection

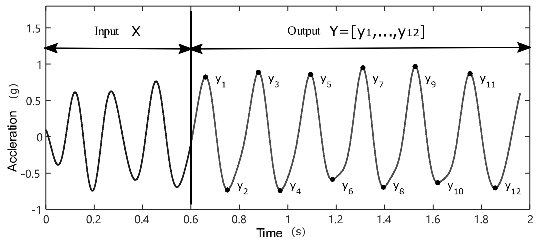

Fig. 10. Pediction principle of small-amplitude hunting

According to the tracking data and the calculated results based on vehicle dynamics, the principal frequencies of the small-amplitude hunting and hunting instability fall within the range of 4~8 Hz. In addition, according to the criteria for hunting instability in China, at least six cycles at these frequencies are required to declare the hunting state. Therefore, a single sample needs to be at least 1.5~2.0 s long.

The focus of this work is to predict variations in small-amplitude hunting based on the LUBE model. Given that the hunting instability is defined by the peak of the lateral acceleration signal of the bogie frame, variations in the state need not be predicted at each point. Therefore, predicting variations of the peaks and troughs suffices.

Fig. 10 presents the transition from small-amplitude hunting to hunting instability. The ordinate is time, and the abscissa is acceleration. With the proposed method, the input lasts

0.6 s for a total of 150 points. Specifically, a raw signal without filtering is used in this method. The output data consist of six cycles of peaks and troughs, for a total of 12 points. The data from the first 0.6 s (blue line) are used to determine whether the current state is a small-amplitude hunting state. At the same time, the same data (blue line) are used to predict the value of 12 points y_1~y_{12} (black points), which allows the evolution of small-amplitude hunting, which will occur in the following 1.4 s, to be predicted by the data of the first 0.6 s.

D. Improving the computational efficiency

If the train is classified as experiencing the hunting instability, an alarm will sound. If the train is classified as being in a normal state, there is no need to predict its evolution. Thus, in this paper, predicting the evolution of the state of a high-speed train focuses on the small-amplitude hunting state.

The prediction model first requires a classifier to determine the current running status of the train. Thus, this algorithm must identify three states: normal, small-amplitude hunting, and hunting instability. If the current state is the small-amplitude hunting state, the algorithm predicts the range of the next peak interval. Finally, the predicted peak range is classified as small-amplitude hunting convergence or divergence, which is determined simply according to the national standard of the hunting instability described in Section 1 of this paper.

Theoretically, no prediction output is required when the hunting is considered normal or already in a hunting instability state. However, in the implementation, classification and prediction are computed simultaneously to improve computational efficiency.

This analysis shows that there is no need to predict the evolution of normal and hunting instability. Therefore, only in the state of small-amplitude hunting is it necessary to process the output results. Note that the prediction interval and the classification result are obtained at the same time which improves the computational efficiency.

Algorithm 1 Pseudocode for computing the final output.

```
Input: Upper interval of prediction (UI), Lower interval of prediction (LI), Classification layer (CL)
Output: Final result
function Final Result (UI, LI, CL)
    if CL is Hunting Instability; return Alarm;
    else if CL is Normal; return 1
    else; return UI and LI
end function
```

In real-time monitoring of train signals, multiple threads are built by this algorithm to avoid data loss and improve computational efficiency. A thread pool is established to manage multiple threads to implement the related logic.

Fig. 11 shows the neural network structure of a model to predict small-amplitude hunting. In this model, the classification and prediction parts are constructed as a single model. The two models share a single convolutional layer parameter, which streamlines the model structure and improves the computational efficiency. This model has two outputs: the classification layer output and the interval-prediction output. Therefore, the model simultaneously classifies and predicts.

E. Neural network structure of model to predict small-amplitude hunting

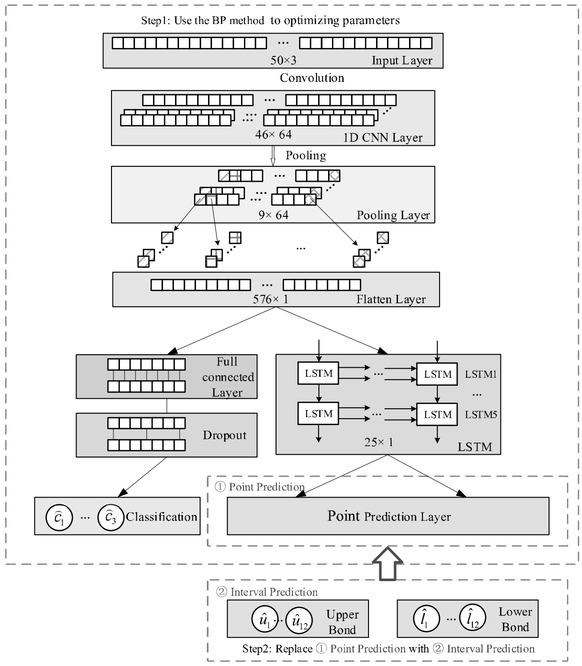

Fig. 11. Neural network structure of model to predict small-amplitude hunting.

TABLE I
PARAMETERS OF MODEL STRUCTURE

Model structure	Layer NO.	Output dimension	Hyper-parameter
Input layer	1	(None, 50, 3)	——
Convolution layer	2	(None, 46, 64)	filters=64, kernel_size=5, activation='relu'
Pooling layer	3	(None, 9, 64)	pool_size=5
Unfold layer	4	(None, 576)	——
LSTM layer	5	(None, 9, 500)	units=500, activation='relu',
	6	(None, 9, 500)	units=500, activation='relu',
	7	(None, 9, 500)	units=500, activation='relu',
	8	(None, 9, 200)	units=200, activation='relu',
	9	(None, 25)	units=25, activation='relu',
Fully connected layer	10	(None, 512)	units=512, activation='relu'
	11	(None, 128)	units=128, activation='relu'
Dropout layer	12	(None, 128)	rate = 0.5
Output layer	13	(None, 12)	units=12, activation='sigmoid'
	14	(None, 12)	units=12, activation= 'sigmoid'
	15	(None, 3)	units=3, activation='softmax'

* 'relu', 'sigmoid', 'softmax' are all activation function.

IV. RESULTS AND DISCUSSION

A. Classification recognition of the small-amplitude hunting

The classification model is trained by leave-one-out cross-validation. The dataset is divided into ten sub-datasets for training, nine of which are used to train the model, and one of which serves to evaluate the performance of the model. This process is repeated ten times. Each of the ten datasets is used once to evaluate the performance of the model. The final accuracy is obtained by computing the average accuracy.
The results given in Table II show that the three operational states of high-speed trains (normal, small-amplitude hunting, and hunting instability) are accurately identified by this classification model. The results also show that the proposed model can classify and accurately identify the status of a high-speed train. In the proposed algorithm, the training set accounts for 60% and the testing machine accounts for 40%.

TABLE II
RESULTS OF SMALL-AMPLITUDE HUNTING RECOGNITION

Category	Normal	Small-amplitude hunting	Hunting
Training sample	60	60	60
Test sample	40	40	40
Accuracy	99.8 %	100%	100%

B. Interval prediction in small-amplitude hunting state

In the overview section of this article, a large number of studies related to PI are introduced. Although these studies are all aimed at various improvements to the LUBE algorithm, they are all based on single-layer hidden layers and cannot meet the demand for hunting prediction in complex high-speed train systems in terms of data robustness. Although both methods in Ref. [41] and Ref. [42] are machine learning methods based on single-layer ELM, they are classic methods used for interval prediction in machine learning. Therefore, this article uses these two methods to compare with TL-LUBE to demonstrate its superiority.

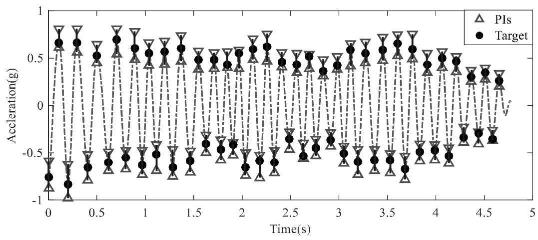

(a) Interval prediction of small-amplitude hunting convergence based on the proposed TL-LUBE method.

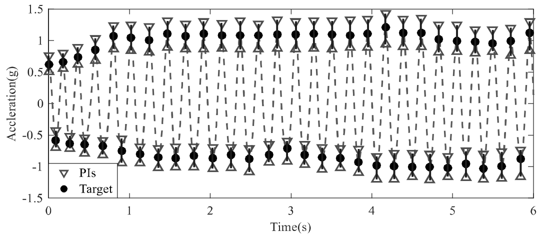

(b) Interval prediction of small-amplitude divergence based on the proposed TL-LUBE method.

Fig. 12. Interval-prediction results for TL-LUBE method

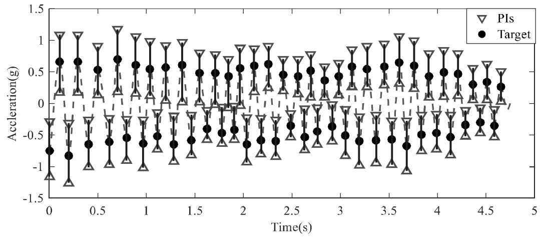

(a) Interval prediction of small-amplitude hunting convergence based on ELM-EL method.

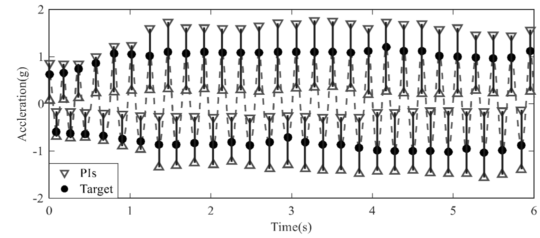

(b) Interval prediction of small-amplitude divergence based on ELM-EL method

Fig. 13. Interval-prediction results for ELM-EL method

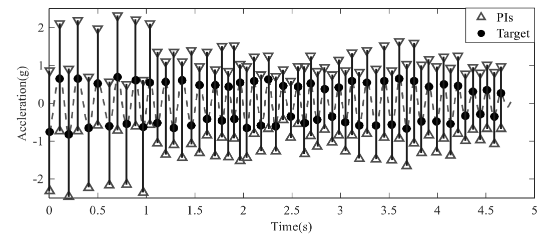

(a) Interval prediction of small-amplitude hunting convergence based on Bootstrap-ELM method

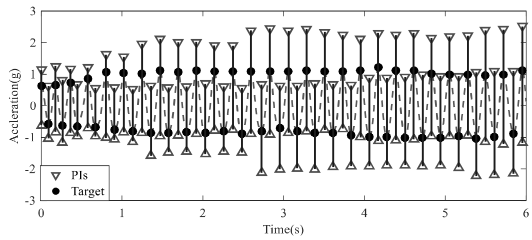

(b) Interval prediction of small-amplitude divergence based on Bootstrap-ELM method

Fig. 14. Interval prediction results for Bootstrap-ELM method

The results displayed in Figs. 12~14 show that a reasonable interval estimation for the evolution of the small-amplitude hunting is obtained by these three methods. The *PICP*s given by the three methods are all close to 100%. However, the *PINAW*s given by the ELM-EL [41] and Bootstrap-ELM [42] methods are excessively large, which may lead to false estimates of hunting.

TABLE III
SMALL-AMPLITUDE HUNTING CONVERGENCE FOR THE THREE METHODS

Method	PICP	PINAW	CWC
TL-LUBE	1	0.104	0.104
ELM-EL	1	0.337	0.337
Bootstrap-ELM	1	1.1462	1.1462

TABLE IV
SMALL-AMPLITUDE DIVERGENCE FOR THE THREE METHODS

Method	PICP	PINAW	CWC
TL-LUBE	1	0.187	0.187
ELM-EL	1	0.578	0.578
Bootstrap-ELM	1	1.373	1.373

As shown in Tables III and IV, the three different methods produce the same *PINAW* and *CWC*, mainly because $PICP = 1$. Based on Eqs. (1) to (6), when $PICP > \mu$ ($\mu = 0.9$), $CWC = PINAW$. Additionally, when each method gives the same *PICP*, the *PINAW* produced by the proposed TL-LUBE model is the smallest: only 32.3% of that of the ELM-EL method and 9.1% of that of the Bootstrap-ELM method. Therefore, the proposed TL-LUBE method performs better than the other two methods presented herein.

In the proposed method, the time required for computing a single sample input is approximately 3.5835×10^{-4} seconds. During high-speed train operation, the unfiltered 250 Hz raw signal (single sample) of the previous 0.6 seconds is input every 0.1 seconds, and the output is the peak and valley information of the acceleration in the future 1.4 seconds, which is equivalent to predicting every 0.1 seconds. Therefore, as long as the time required for computing a single sample input in the model is less than 0.1 seconds, it can meet the requirements for online monitoring of long-term forecasting.

In short, the results lead to the following conclusions:

1) The proposed TL-LUBE method can be used to predict the evolution of the small-amplitude hunting state.
2) The proposed TL-LUBE method provides more accurate predictions than the ELM-EL or Bootstrap-ELM methods.

V. CONCLUSIONS

1) The evolution of small-amplitude hunting is studied to predict the occurrence of the hunting instability in this work.
2) A TL-LUBE model is proposed herein to improve the parameter optimization of the LUBE. The parameters of this model are divided into primary and secondary networks; the parameters of the primary network are trained by using the gradient descent method, and the parameters of the secondary model are optimized by using a heuristic algorithm.
3) It is necessary to identify the small-amplitude hunting state before predicting the changing trend of the small-amplitude hunting. However, the method of classifying first and then predicting tends to over-complicate the model because the classification and prediction models must be separately constructed, leading to low computational efficiency. Therefore, in the proposed model, the classification and prediction models are combined, and the two models share a single convolutional layer parameter, which streamlines the model structure and improves the computational efficiency. Thus, the classification (normal, small-amplitude hunting, or hunting instability) and prediction (interval prediction for the small-amplitude hunting) are implemented simultaneously to improve the computational efficiency

The proposed method can be applicated in other fault diagnosis fields, such as prediction of the wind speed.

The data from high-speed trains were obtained by experimentation. The fault and normal data were unbalanced in the actual testing data. Therefore, in future research, the vehicle dynamics simulation model and the measured tracking data set should be studied together. The simulation data generated by the vehicle dynamics model can then be used to analyze the evolution of small-amplitude hunting.

REFERENCES

[1] Y. He, J. Wu, Y. Zheng, Y. Zhang, X. Hong, “Track defect detection for high-speed Maglev trains via deep learning,” *IEEE Transactions on Instrumentation and Measurement*, vol. 71, pp. 1-8, 2022, Art no. 3506008.

[2] S. Gao, “Automatic detection and monitoring system of pantograph–catenary in China’s high-speed railways,” *IEEE Transactions on Instrumentation and Measurement*, vol. 70, pp. 1-12, 2021, Art no. 3502012.

[3] Y. Zhang, N. Qin, D. Huang, J. Du, “Precise diagnosis of unknown fault of high-speed train bogie using novel FBM-Net,” *IEEE Transactions on Instrumentation and Measurement*, vol. 71, pp. 1-11, 2022.

[4] J. Sun, M. Chi, W. Cai, X. Jin, “Numerical investigation into the critical speed and frequency of the hunting motion in railway vehicle system,” *Mathematical Problems in Engineering*, vol. 2019, pp.1-15, Apr. 2019, Art. no. 7163732.

[5] C. Uyulan, M. Gokasan, S. Bogosyan, “Dynamic investigation of the hunting motion of a railway bogie in a curved track via bifurcation analysis,” *Mathematical Problems in Engineering*, vol. 2017, pp. 1–15, Jul. 2017, Art. no. 8276245.

[6] A. Rahmati-Alaei, M. Sharavi, M. Samadian Zakaria, “Hunting stability analysis of partially filled tank wagon on curved track using coupled CFD-MBD method,” *Multibody System Dynamics*, vol. 50, pp.45-69, 2020.

[7] D. Skerman, C. Cole, M. Spiryagin, “Determining the critical speed for hunting of three-piece freight bogies: practice versus simulation approaches,” *Vehicle System Dynamics*, vol. 60, no. 10, pp. 3314-3335, 2022.

[8] Y. Yamanaga, K. Kido, “Influence of excitation condition on evaluating critical hunting speed,” *Quarterly Report of RTRI*, vol. 60, no. 2, pp. 97-102, May. 2019.

[9] V. Kumar, V. Rastogi, P. M. Pathak, “Modelling and evaluation of the hunting behaviour of a high-speed railway vehicle on curved track,” *Proceedings of the Institution of Mechanical Engineers, Part F: Journal of Rail and Rapid Transit*, vol. 233, no. 2, pp. 220-236, Feb. 2019.

[10]K. Kritikakos, S.D. Fassois, J.S. Sakellariou, I. Chronopoulos, A. Deloukas, I.A. Iliopoulos, G. Leoutsakos, I. Tountas, G. Vlachospyros, “On the problem of on-board early detection of hunting on rail vehicles: an exploratory study,” *IFAC-PapersOnLine*, vol. 54, no. 20, pp. 191-197, 2021.

[11]H. Ji, “Optimization-based incipient fault isolation for the high-speed train air brake system,” *IEEE Transactions on Instrumentation and Measurement*, vol. 71, pp. 1-9, 2022, Art no. 3501709.

[12]Y. Wu, W. Jin, Y. Li, D. Wang, “A novel method for simultaneous-fault diagnosis based on between-class learning,” *Measurement*, vol. 172, Feb. 2021, Art. no. 108839.

[13]Railway applications-testing for the acceptance of running characteristics of railway vehicles-Testing of running behavior and stationary tests, BS EN 14363, 2005.

[14]Vehicle/Track Interaction Safety Standards, FRA Docket Number 2013-0469, 2013.

[15]Concerning a technical specification for interoperability relating to rolling stock sub-system of the trans- European high-speed rail system, 2008/232/EC, 2008.

[16]D. Huang, S. Li, N. Qin, Y. Zhang, “Fault diagnosis of high-speed train bogie based on the improved-CEEMDAN and 1-D CNN algorithms,” *IEEE Transactions on Instrumentation and Measurement*, vol. 70, pp. 1-11, 2021, Art no. 3508811.

[17]L. Chen, N. Qin, X. Dai, D. Huang, “Fault diagnosis of high-speed train bogie based on capsule network,” *IEEE Transactions on Instrumentation and Measurement*, vol. 69, no. 9, Sep. 2020.

[18]Q. Lu, R. Yang, M. Zhong, Y. Wang, "An improved fault diagnosis method of rotating machinery using sensitive features and RLS-BP neural network," *IEEE Transactions on Instrumentation and Measurement*, vol. 69, no. 4, pp. 1585-1593, Apr. 2020.
[19]Specification for dynamic performance assessment and testing verification of rolling stock, GB/T 5599-2019, 2019.
[20]A.F.D. Souza, P. Caravavatna, T Wang, "Nonlinear analysis of bogie serpentine vibration," *Foreign Rolling Stock*, vol. 4, pp. 5-14, 1986.
[21]H. True, C.K. Petersen, "A bifurcation analysis of nonlinear oscillations in railway vehicles," *Vehicle System Dynamics*, vol. 12, no. 1-3, pp. 5-6, 1983.
[22]W.J.V.S.D. Kik, "Comparison of the behaviour of different wheelset-track models," *Vehicle System Dynamics*, vol. 20, pp. 325-339, 1992.
[23]S. Qu, J. Wang, D. Zhang, D. Li, L. Wei, "Failure analysis on bogie frame with fatigue cracks caused by hunting instability," *Engineering Failure Analysis*, vol. 128, pp. 1-11, Oct. 2021.
[24]L. Sun, J. Yao, "Hunting derailment safety evaluation method of high-speed railway vehicle," *China Railway Science*, vol. 34, no. 5, pp. 82-92, Sep. 2013.
[25]W. An, R. Wu, J. Shi, F. Gan, Y. Qi, "Research on hunting instability monitoring system of high speed freight bogie", *IOP Conference Series: Materials Science and Engineering*, vol. 790, no. 1, pp. 1-7, 2020.
[26]J. Yao, L. Sun, F. Hou, "Study on evaluation methods for lateral stability of high-speed trains," *China Railway Science*, vol. 33, no. 6, pp. 132-139, Nov. 2012.
[27]D. Gan, "Recognition method and real-time online monitoring device for lateral stability of high speed train based on Bayesian clustering," C*hina Railway Science*, vol. 37, no. 4, pp. 139-144, Jul. 2016.
[28]Y. Zeng, W. Zhang, D. Song, "A new strategy for hunting alarm and stability evaluation for railway vehicles based on nonlinear dynamics analysis," *Proceedings of the Institution of Mechanical Engineers Part F-Journal of Rail and Rapid Transit*, vol. 234, no. 1, pp. 54-64, Jan. 2020.
[29]J. Sun, E. Meli, W. Cai, H. Gao, M. Chi, A. Rindi, S. Liang, "A signal analysis based hunting instability detection methodology for high-speed railway vehicles," *Vehicle System Dynamics*, vol. 59, no. 10, pp. 1461-1483, 2021.
[30]J. Ning, Q. Liu, H. Ouyang, C. Chen, B. Zhang, "A multi-sensor fusion framework for detecting small amplitude hunting of high-speed trains," *Journal of Vibration and Control*, vol. 24, no. 17, pp. 3797-3808, 2018.
[31]J. Ning, M. Fang, W. Ran, C. Chen, Y. Li, "Rapid multi-sensor feature fusion based on non-stationary kernel JADE for the small-amplitude hunting monitoring of high-speed trains," *Sensors*, vol. 20, no. 3457, pp. 1-17, Jun. 2020.
[32]J. Ning, W. Cui, C. Chong, H. Ouyang, C. Chen, B. Zhang, "Feature recognition of small amplitude hunting signals based on the MPE-LTSA in high-speed trains," *Measurement*, vol. 131, pp. 452-460, 2018.
[33]Y. Ye, J. Ning, "Small-amplitude hunting diagnosis method of high-speed trains based on bogie frame's lateral-longitudinal-vertical data fusion, Independent mode function reconstruction and linear local tangent space alignment," *Proceedings of the Institution of Mechanical Engineers, Part F: Journal of Rail and Rapid Transit*, vol. 233, no. 10, pp. 1050-1067, 2019.
[34]H. Chen, B. Jiang, "A review of fault detection and diagnosis for the traction system in high-speed trains," *IEEE Transactions on Intelligent Transportation Systems*, vol. 21, no. 2, pp. 450-465, Feb. 2020.
[35]A. Khosravi, S. Nahavandi, D. Creighton, A.F. Atiya, "Lower upper bound estimation method for construction of neural network-based prediction intervals," *IEEE Transactions on Neural Networks*, vol. 22, no. 3, pp. 337-346, Mar. 2011.
[36]Z. Gan, C. Li, J. Zhou, G. Tang, "Temporal convolutional networks interval prediction model for wind speed forecasting," *Electric Power Systems Research*, vol. 191, no. 106865, pp. 1-10, Feb. 2021.
[37]C. Lian, Z. Zeng, X. Wang, W. Yao, Y. Su, H.M. Tang, "Landslide displacement interval prediction using lower upper bound estimation method with pre-trained random vector functional link network initialization," *Neural Networks*, vol. 130, pp. 286-296, Oct. 2020.
[38]P. Li, C. Zhang, H. Long, "Solar power interval prediction via lower and upper bound estimate on with a new model initialization approach," *Energies*, vol. 12, no. 21, pp. 4146, Oct. 2019.
[39]Q. Li, J. Wang, H. Zhang, "A wind speed interval forecasting system based on constrained lower upper bound estimation and parallel feature selection," *Knowledge-Based Systems*, vol. 231, no. 107435, pp. 1-19, Nov. 2021.
[40]J. Lu, J. Ding, "Construction of prediction intervals for carbon residual of crude oil based on deep stochastic configuration networks," *Information Sciences*, vol. 486, pp. 119-132, Jun. 2019.
[41]Q. Ni, S. Zhuang, H. Sheng, G. Kang, J. Xiao, "An ensemble prediction intervals app Optimal Uncertainty-guided Neural Network Training roach for short-term PV power forecasting," *Energies*, vol. 155, pp. 1072-1083, Oct. 2017.
[42]X. Qi, K. Li, X. Yu, Z. Zhang, J. Lou, "Transformer top oil temperature interval prediction based on kernel extreme learning machine and bootstrap method," *Proceedings of the Chinese Society of Electrical Engineering*, vol. 37, no. 19, pp. 5821-5828, Oct. 2017.
[43]Z. Shi, H. Liang, V. Dinavahi, "Direct interval forecast of uncertain wind power based on recurrent neural networks," *IEEE Transactions on Sustainable Energy*, vol. 9, no. 3, pp. 1177-1187, Jul. 2018.
[44]A. Kavousi-Fard, A. Khosravi, S. Nahavandi, "Reactive power compensation in electric arc furnaces using prediction intervals," I*EEE Transactions on Industrial Electronics*, vol. 64, no. 7, pp. 5295-5304, Jul. 2017.
[45]C. Lian, L. Zhu, Z. Zeng, Y. Su, W. Yao, H. Tang, "Constructing prediction intervals for landslide displacement using bootstrapping random vector functional link networks selective ensemble with neural networks switched," *Neurocomputing*, vol. 291, pp. 1-10, May. 2018.
[46]F. Liu, C. Li, Y. Xu, G. Tang, Y. Xie, "A new lower and upper bound estimation model using gradient descend training method for wind speed interval prediction," *Wind Energy*, vol. 24, no. 3, pp. 290-304, 2021.
[47]X. Peng, Q Xu, H. Wang, J. Lang, W. Li, T. Cai, S. Duan, Y. Xie, C. Li, "A novel efficient DLUBE model constructed by error interval coefficients for clustered wind power prediction," *IEEE Access*, vol. 9, pp. 61739-61751, Apr. 2021.
[48]H. M. D. Kabir, A. Khosravi, A. Kavousi-Fard, S. Nahavandi, D. Srinivasan, "Optimal uncertainty-guided neural network training," *Applied Soft Computing*, vol. 99, 2021.
[49]A. Saeed, C. Li, Z. Gan, "Short-term wind speed interval prediction using LUBE based quasi-recurrent neural network", *Journal of Physics: Conference Series*, vol. 2189, no. 1, 2022.
[50]S. Mirjalili, "Dragonfly algorithm: a new meta-heuristic optimization technique for solving single-objective, discrete, and multi-objective problems," *Neural Computing & Applications*, vol. 27, no. 4, pp. 1053-1073, May. 2016.
[51]W. Alan, S. Jack B., S. Harry L., V. John A., "Determining lyapunov exponents from a time series," *Physica D: Nonlinear Phenomena*, vol. 16, no. 3, pp. 285-317, Jul. 1985.

Jing Ning received Ph. D degree in Information Science and Technology from Southwest Jiaotong University, Chengdu, China, in 2011. She is currently an Assistant Professor at Southwest Jiaotong University. She is engaged in scientific research on failure behavior analysis under high-speed train operating conditions, and is very familiar with the related theories of high-speed train hunting motion and the structure of high-speed train running parts.

Mingkuan Fang received the Master's degree in Mechanical Engineering from Southwest Jiaotong University, Chengdu, China. His current research interests include High-speed train small-amplitude hunting state detection and time series-analysis.

Duoying Wang received the B.S. degree in Mechanical Engineering from Southwest Jiaotong University, Chengdu, China. He is· currently working toward the Master's degree in Southwest Jiaotong University, Chengdu, China. His current research interests include High-speed train small-amplitude hunting state detection and transfer learning.

Chunjun Chen born in 1967, Doctor of Engineering and Professor in China. In 1993, he joined Southwest Jiaotong University, Chengdu, China, where he is currently a Professor in the Faculty of Mechanical Engineering. His research interests lie in the fields of vibration, noise, and air dynamic analysis of high-speed train and performance tests and active control of transportation equipment. Taking high-speed train as the research subject in the long run, he does researches on train aerodynamic performance tests, inside pressure fluctuation tests, vibration tests, vibration active/ semi-active controls, modern signal processing, numerical simulation and line tests.

Huajiang Ouyang is currently a full Professor at the School of Engineering in the University of Liverpool and the Head of the Dynamics and Control Group. He received BEng and MSc in Engineering Mechanics in 1982 and 1985, respectively, and PhD in Structural Engineering in 1989, at Dalian University of Technology. Prof. Ouyang is also a Fellow of Institute of Physics and a Fellow of Higher Education Academy. He was a Royal Academy of Engineering and Leverhulme Trust Senior Research Fellow in 2009-2010. He also is a Changjiang Chair Professor in China. His main research areas are structural dynamics and control, and structural identification. He is particularly interested in friction-induce vibration, moving-load dynamics, inverse structural modifications, and vibration-based energy harvesting. He has published 280+ journal papers and 110+ conference papers.